Materials Characterization 158 (2019) 109934

Contents lists available at ScienceDirect

Materials Characterization

journal homepage: www.elsevier.com/locate/matchar

Microstructure and micro-hardness behavior of Ti–Y_2O_3 –Al–Si composite coatings prepared in electron-plasma alloying

Dmitrii Zaguliaev[a,b], Sergey Konovalov[a,c,*], Yurii Ivanov[d], Viktor Gromov[b]

[a] Institute of Laser and Optoelectronic Intelligent Manufacturing, Wenzhou University, No. 19 Binhai 3rd Road, Yongxing Street, Longwan District, Wenzhou, Zhejiang, 325024, China

[b] Siberian State Industrial University, 42, Kirov St., Novokuznetsk, 654007, Russia

[c] Samara National Research University, 34, Moskovskoye Shosse, Samara, 443086, Russia

[d] Institute of High Current Electronics, Siberian Branch, Russian Academy of Sciences, 2/3 Akademichesky Avenue, Tomsk, 634055, Russia

ARTICLE INFO

Keywords:
Al-11%Si alloy
Electron-plasma alloying
Surface
Microstructure
Micro-hardness

ABSTRACT

The paper investigates micro-hardness behavior, element and phase composition of Al–11%Si compound subjected to electron-plasma alloying (EPA). Essentially, EPA is an electrical explosion of a Ti conductor and a weighted Y_2O_3 powder sample with further high-speed heating created by an intense pulse electron beam. The work has established a considerable increase in micro-hardness in surface layers of the material. A penetration depth of alloying elements, being a thickness characteristic of the modified layer, is reported to be ~170 μm. A maximal micro-hardness (155 ± 15.5 HV) is detected in a layer to be as close as possible (5 μm) to the surface of modification. Micro-hardness drops gradually at a depth of 110 μm, reaching its initial value 85.9 ± 8 HV at a depth of 170 μm. The research data collected by the methods of X-ray microanalysis and transmission electron diffraction microscopy demonstrate that the structure of EPA-treated composite 5 μm below the surface comprises nano-dimensional (1–100 nm) crystallites composed mainly of aluminum. The study has revealed that in some crystallites and their joining points there are inclusions formed by particles of Ti and Y aluminides (Al_3Ti and Y_3Al_2) and Ti silicides ($TiSi_2$). The structure of alloy ≈70 μm below the treated surface is made of high-speed crystallization cells ranging 0.5 μm–0.6 μm. The crystallization cells are shown to be formed by a solid Al-based solution and surrounded by second phase layers containing Si and $Cu_{2.7}Fe_{6.3}Si$; cross dimensions of which vary 50–70 nm. A comparison of micro-hardness behavior and concentration of alloying elements in the surface layer of the composite has highlighted a boost of micro-hardness caused by Ti and Y in the modified layer, and multiphase sub-micro-and nano-dimensional structure made of crystallites with dimensions within a range of several units to hundreds of nanometers.

1. Introduction

To date, there is a large volume of published theoretical and experimental studies describing aluminum alloys due to their technological and industrial significance. Casting alloys are the most essential ones in industry, i.e. a percentage of alloys Al–Si in a total number of castings is above 90% [1]. This fact is purely caused by their outstanding casting characteristics, cracking resistance and good processing parameters nearly for all casting techniques. However, a low strength hardly furthers their wider industrial application. As a consequence, new manufacturing processes of alloys with better mechanical properties have been developed. Powder metallurgy [2], the use of different external fields in the process of crystallization [3,4] and high plastic deformations [5] are thought to be new manufacturing methods of high strength aluminum alloys. The works [6,7] research the effect of thermal treatment and introduction of alloying elements on the microstructure and mechanical properties of Al–Si–Cu and Al–Si–Mg composite. The studies have established that introduction of alloying elements and thermal treatment carried out simultaneously dissolve intermetallic phases, make distribution of alloying elements in the matrix more homogenous and improve strength characteristics of composites. Mostly, a comprehensive hardening of the material is not needed, and it is sufficient to modify thin layers (around 200 μm) only, which have to resist to different stresses. Modification of surface layers without any changes in structure and chemical composition of the material includes plasma deposition of wear resistant coatings [8], electron or laser

* Corresponding author. Institute of Laser and Optoelectronic Intelligent Manufacturing, Wenzhou University, No. 19 Binhai 3rd Road, Yongxing Street, Longwan District, Wenzhou, Zhejiang, 325024, China.,

E-mail addresses: ksv@ssau.ru, ksv@edu.wzu.cn (S. Konovalov).

https://doi.org/10.1016/j.matchar.2019.109934
Received 3 July 2019; Received in revised form 8 September 2019; Accepted 14 September 2019
Available online 25 October 2019

irradiation [9–11], and a combination of these methods as well [12]. In certain circumstances, e.g. in high-duty machine parts and equipment components a surface of material with high-grade performance characteristics is to be formed. As traditional methods of strengthening can't solve this problem, researchers have to look for new approaches to improve structure and properties. A combination of several modification procedures is a prospective field in this case, for instance, electron-plasma alloying (EPA) combining electrical explosion, followed by treatment with an intense pulsed electron beam. In our opinion, a more uniform overlayer with much improved performance characteristics can be deposited due to better melting of the material surface provided that coatings deposited in electrical explosion are treated by intense electron beams [13,14].

A hypoeutectic Al–11%Si alloy is one of the most common casting aluminum composites to contain additional alloying elements Cu, Mg and Ni and applied in motor-car industry for manufacturing pistons. In operation of the internal combustion engine pistons move in sliding friction conditions, i.e. a piston skirt rubs against a cylinder made normally of a stronger material. Unavoidably, this process causes wear of the piston skirt with further formation of scratch marks on its surface. So, in this case a surface treatment is thought to be quite suitable, since an entire modification of the alloy is not required. Ti is considered to be a future material for the surface treatment because its strength characteristics are far better than strength of Al–11%Si alloy. Titanium-based alloys have been in the focus of researchers so far, it has been found that titanium coatings deposited on aluminum base improves its strength enormously [15,16].

This work aims at investigating structure and micro-hardness of Al–11%Si composite alloy subjected to electron-plasma alloying and revealing regularities of these processes.

2. Material and methods

Casting alloy Al–11%Si was used for the purpose of research. Its chemical composition was determined by means of X-ray microanalysis (wt %): Al – 84.88, Si – 11.10, Cu – 2.19, Ni – 0.92, Mg – 0.58, Fe – 0.25, Ti – 0.05, Mn – 0.02, Cr – 0.01. The surface layer was modified via electric current explosion (discharge voltage 2.6 kV) [17] of Ti conductor (58.9 mg) and adding a weighted powder portion Y_2O_3 (88.3 mg) to a plasma jet.

When a storage capacitor discharges, a high-density electrical current flows in electrodes through a conductor to be exploded (Ti foil), causing its explosion this way. Explosion products are forced into a vacuum processing chamber (a residual pressure of 100 Pa), carrying particles of Y_2O_3 powder weighted portion. A sample is placed into a vacuum processing chamber at various distances from the nozzle and fixed by a sample holder. The products of electrical explosion are a multiphase system composed of a plasma component (Al) and condensed particles of different dispersion (Y_2O_3), which precipitate on the surface of an item to be treated, so a multi-component coating is formed. A flowing onto the surface and returning supersonic front of the jet causes the formation of a shocked layer with high temperature and pressure. So, the surface is heated up to and above the temperature of melting in a short exposure period to pulsed plasma.

A coating obtained as a result of explosion was heated by intense electron beam (energy of accelerated electrons – 17 keV, electron beam pulse duration – 150 μs, number of pulses – 3, density of electron beam energy – 35 J/cm^2) at a high speed [18]. Electron-plasma alloying (EPA) is a combination of high energy treatments.

For the purpose of research five plates of a size 20 × 20 × 10 mm^3 were used. A plane 20 × 20 mm^2 of samples was oriented perpendicular to the axis of a plasma jet generated in electrical explosion. A beam of electrons was applied along the normal to the same plane. The pattern of main alloying elements was assessed 5 times for each depth.

Optimal parameters of electric explosion and electron beam treatment to form unique gradient, multi-element, multiphase, nano-

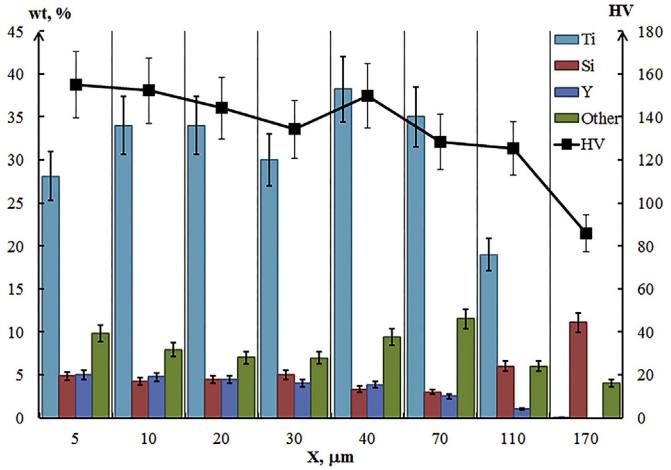

Fig. 1. Main alloying elements (wt. %) and microhardness (HV) in layers of Al–11%Si composite at different depths (X, μm) from EPA-modified surface.

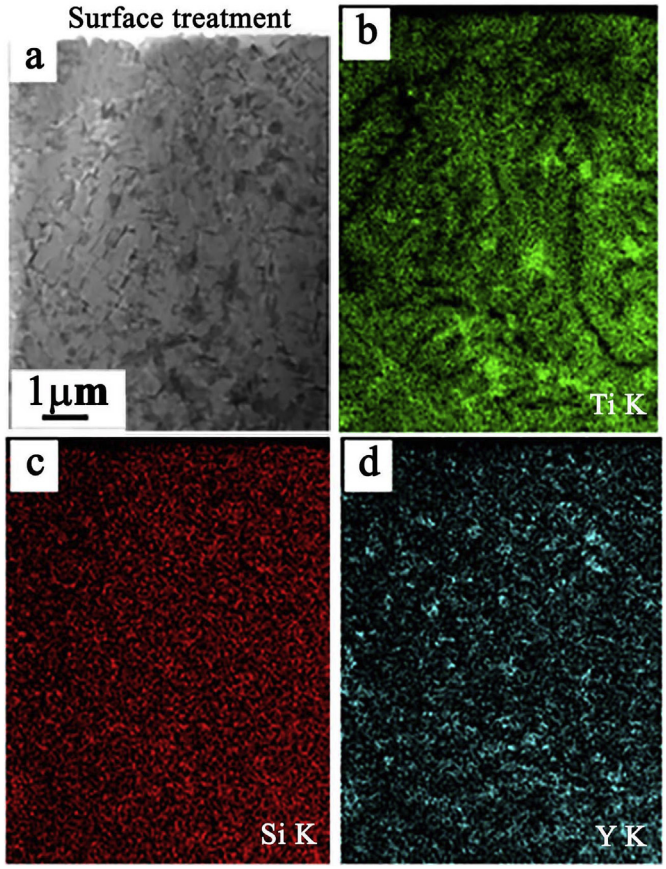

Fig. 2. Electron-microscopic (bright field) image of the modified layer structure in Al–11%Si composite to be adjacent to the EPA-treated surface (a); b-d – images of foil sections taken in a characteristic X-ray emission.

structural states in the modified layer were previously determined for each type of energy deposition [17,18].

Element and phase composition, state of the defect substructure was studied using transmission electron microscopy (device JEM 2100F) and X-ray diffraction analysis (Shimadzu XRD 6000 X-ray diffractometer) [20–22].

Foils to explore structural and phase states of the material were cut near the treated surface via electro-spark method. At least three foils were used at each distance from the surface under study (5 μm and

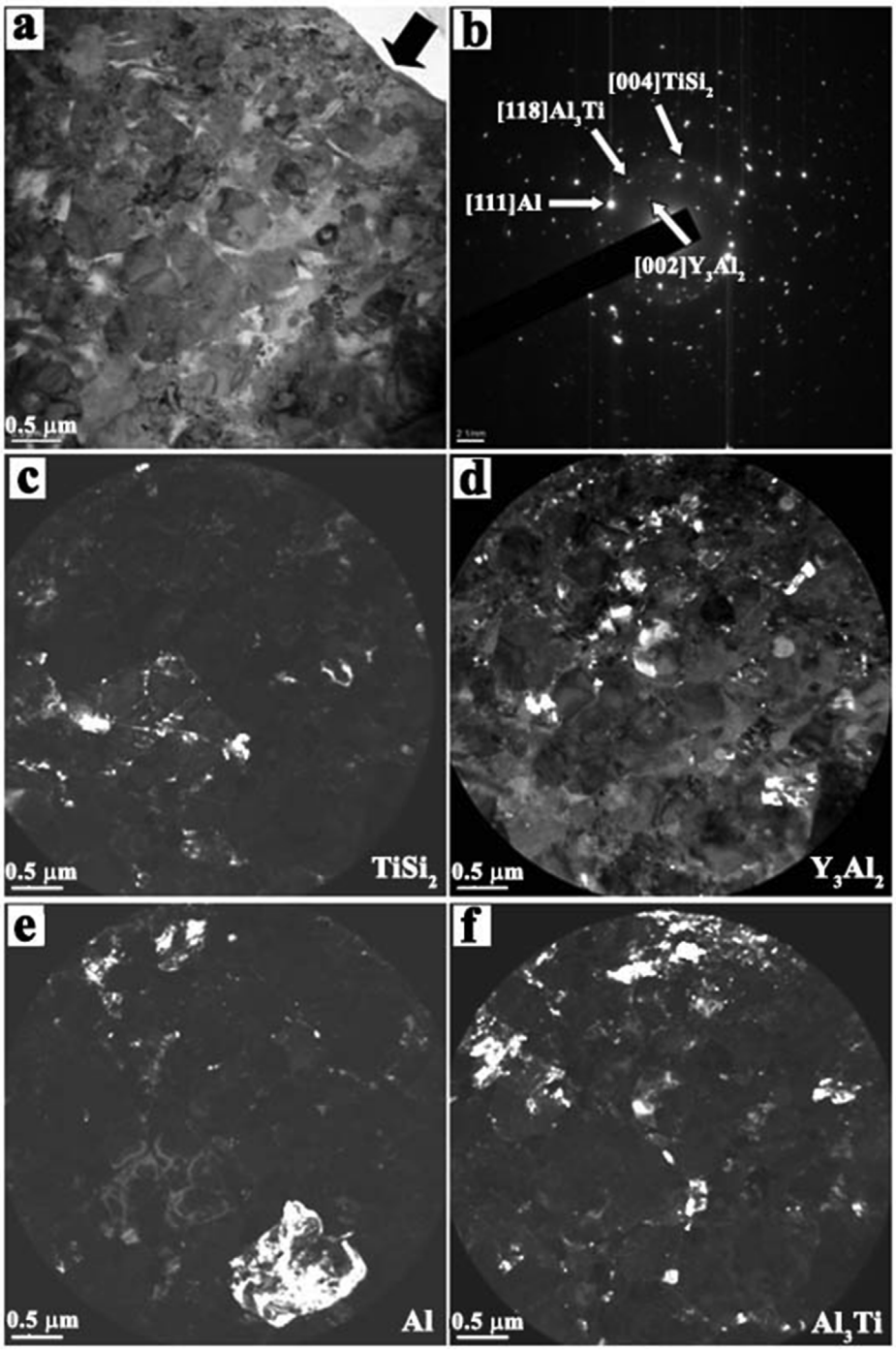

Fig. 3. Electron-microscopic (bright field) image of the modified layer structure in Al–11%Si alloy to be adjacent to the EPA-treated surface; a –bright field image; b – SAED; c-f – dark fields obtained in reflexes [004]$TiSi_2$, [002]Y_3Al_2, [111]Al, [118]Al_3Ti; arrows indicate: (a) – a surface of modification, (b) – reflexes, where dark fields are obtained.

70 μm) for five samples. The most characteristic electron microscopic images are presented in (Figs. 2–5). Selecting a cutting mode, it was necessary to avoid extra deformation, preventing from damaging a structure of the sample. So, plates with a thickness of 100 μm were thinned in ion etching (device IonSlicer EM-09100IS). Samples for IonSlicer were prepared as a parallelepiped $2.8 \times 0.5 \times 0.1$ mm, then covered with a special protecting tape and thinned by argon ion beam. Energy of the beam was below 8 kW and an angle of incidence was varied 0^0 to 6^0 towards the largest facet of the sample. It minimizes irradiation-related damage and preserves original structure and phase composition of the sample for further studies by transmission electron microscopy methods.

Vickers micro-hardness of samples was measured according to the technique given in International Standard ISO 6507:2005 by a HVS-1000 micro-hardness tester using a four-sided diamond pyramid with a square base, in conditions: indenter load 0.5 N, time of loading and retention 10 s, unloading time 5 s.

3. Results and discussion

Fig. 1 shows an average distribution pattern of main alloying elements developed according to data of X-ray diffraction analysis

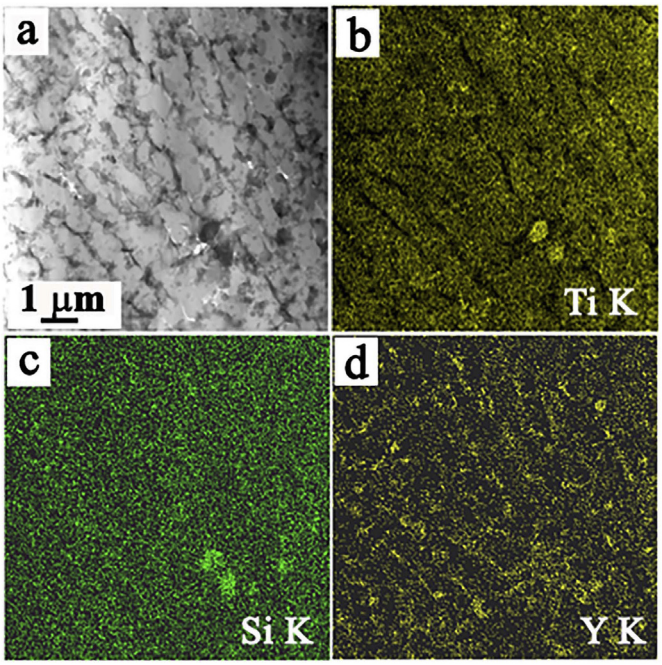

Fig. 4. Electron-microscopic (bright field) image of the modified layer structure in Al–11%Si alloy 70 μm below the treated surface (a); b-d – images of foil sections taken in a characteristic X-ray emission.

obtained in the study of three samples and micro-hardness behavior with regard to a depth from the EPA-treated surface.

A thickness of the alloyed layer, i.e. layer with detected alloying elements not to be found in as cast silumin (titanium, yttrium) is seen to be around 110 μm. It stands to mention that Ti is a prevalent alloying element in the modified layer. An amount of Ti ranges 19 wt% at a depth of 110 μm to 38.24 wt.% at a depth of 40 μm, there are no alloying elements of plasma jet (Ti, Y) detected below 110 μm. A concentration of Y drops in a monotonous way, being zero at depths below 110 μm. Si concentration doesn't exceed 5 wt.% 5–70 μm below the surface, increasing, however, to 11 wt.% being similar to chemical composition of as cast alloy if measured below this depth. The relation between a sum concentration of other alloying elements (Cu, Ni, Mg, Fe, Mn, Cr) and distance to the surface to be modified is non-monotonous. Analyzing deeper in the matter, the concentration drops in a range of 0–30 μm. It increase at distances ranging 30–170 μm with a subsequent decrease, being maximal at a depth of 70 μm. No significant change in concentration of other alloying elements is registered in the composite, since it ranges max 5 wt. %.

Analyzing micro-hardness with regard to the depth from the modified surface we found its maximal value (155 ± 15.5 HV) in the nearest layer to the surface, 5 μm. At depths above 30 μm a monotonous decline of micro-hardness is detected, a slight rise of micro-hardness (150 ± 14.9 HV) is revealed at a depth of 40 μm, then, it falls to 85.9 ± 8 HV at a depth of 170 μm, being typical for as cast Al–11%Si alloy.

Comparing micro-hardness behavior vs. depth from the modified surface and concentration of alloying elements we concluded that micro-hardness increases due to Ti and Y in the modified layer, because micro-hardness at a depth 170 μm, where alloying elements mentioned above are not found, is similar to micro-hardness of as cast alloy. Interestingly, Ti concentration vs. depth from the modified layer correlates with the micro-hardness behavior.

Since a maximal micro-hardness (155 ± 15.5 HV) is found in a layer at a depth of 5 μm, and a sharp drop of micro-hardness and concentration of alloying elements is detected at a depth of 70 μm and deeper, these zones of the alloy were subjected to transmission electron microscopic analysis [19,20] and X-ray microanalysis based on mapping [23].

X-ray microanalysis, namely, mapping procedure makes it possible to visualize a pattern of chemical elements in the modified layer of Al–11%Si alloy. Fig. 2 demonstrates research data on distribution of Ti, Si and Y atoms in the layer adjacent to the EPA-modified surface. A closer inspection of images shows inhomogeneous distribution of elements above, and inclusions of various shapes and dimensions. It is noteworthy that such structure is registered in a layer above 40 μm.

Fig. 3 provides results of micro-diffraction electron-microscopic study on the surface layer in alloy under consideration (a surface to be modified is indicated with an arrow in Fig. 3a). It is clear that dimensions of crystallites in the layer to be studied range from units to hundreds of nanometers; so, the modified layer is a sub-micro nanocrystalline material. Dark-field analysis data on phase composition in the layer are given in Fig. 3c–d. As seen in electron-diffraction micropatterns, sub-micron crystallites are made of solid aluminum-based solution (Fig. 3e). Nano-dimensional inclusions are formed by particles of Ti and Y aluminides (Al_3Ti and Y_3Al_2) (Fig. 3d, f), as well as by Ti silicides ($TiSi_2$) (Fig. 3c).

According to outcomes of X-ray microanalysis a layer of material with a cellular crystallization structure saturated with Al and Ti atoms is found 70 μm below the treated surface (Fig. 4a, c). Crystallization cells are surrounded by second phase layers saturated with Y atoms (Fig. 4d). A homogenous pattern of Si is detected in the material (Fig. 4c).

Fig. 5 demonstrates data on micro-diffraction electron-microscopic study on a layer ≈70 μm below the treated surface. A closer inspection of the Figure indicates cells of high-speed crystallization. Dimensions of the cells are in a range 0.5–0.6 μm. The electron diffraction micropattern (Fig. 5c) shows that crystallization cells are formed by a solid aluminum-based solution (Fig. 5d). The cells are separated by second phase layers containing Si and $Cu_{2,7}Fe_{6,3}Si$ (Fig. 5e–f), the cross sizes of which are in a range 50–70 nm.

4. Conclusions

To sum up, using transmission electron diffraction microscopy of thin foils we investigated element and phase composition of Al–11%Si composite to be EPA-modified. The point of EPA is an electric explosion with a weighted powder portion and subsequent heating by intense pulse electron beam. A thickness of the modified layer, i.e. a layer with alloying elements (Ti, Y) was determined to be ˜170 μm. The modified layer is distinguished by higher micro-hardness, with its maximum (155 ± 15.5 HV) being in the nearest layer to the surface (5 μm). Comparing micro-hardness behavior vs. depth from the modified surface and concentration of alloying elements we concluded that micro-hardness increases due to Ti and Y in the modified layer, because micro-hardness at a depth of 170 μm, where alloying elements mentioned above are not found, is similar to micro-hardness of as cast alloy. The study highlighted that, as a result of EPA, a multiphase sub-micro nano-dimensional state is formed in the surface layer of the material under consideration, and its crystallites vary in a range from units to hundreds of nanometers, being an additional factor to explain the increase in micro-hardness.

Data availability statement

The raw/processed data required to reproduce these findings cannot be shared at this time as the data also forms part of an ongoing study.

Acknowledgements

This work was supported by the Ministry of Science and Higher Education of the Russian Federation [state contract No. 3.1283.2017/4.6] and partially supported by the Russian Foundation for Basic

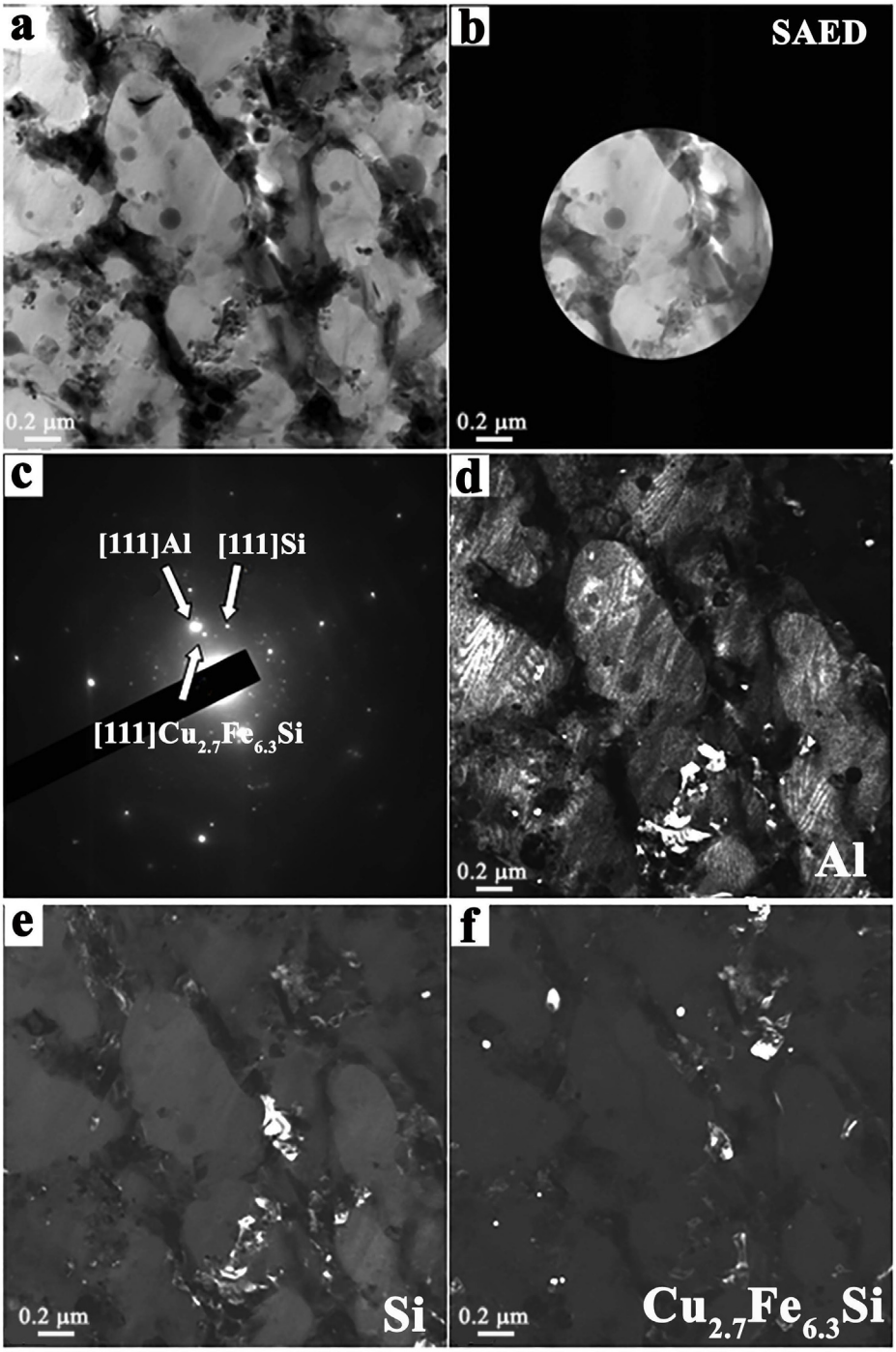

Fig. 5. Electron-microscopic image of the structure in Al–11%Si alloy 70 μm below the treated surface; a-c – bright field image with SAED; d-f – dark field obtained in reflexes [111]Al + [302]Si, [111]Si, [111]$Cu_{2,7}Fe_{6,3}Si$, respectively; arrows (b) indicate the reflexes, where dark fields are obtained.

Research [project No. 19-48-700010]. The authors are grateful to E. Petrikova and A. Teresov for assistance in obtaining and discussing results.

Appendix A. Supplementary data

Supplementary data to this article can be found online at https://doi.org/10.1016/j.matchar.2019.109934.

References

[1] M.V. Glazoff, A.V. Khvan, V.S. Zolotorevsky, N.A. Belov, A.T. Dinsdale, Industrial and perspective casting alloys, Casting Aluminum Alloys, Butterworth-Heinemann, Elsevier Ltd., 2019, pp. 405–510.

[2] S. Whalen, M. Olszta, C. Roach, J. Darsell, D. Graff, Md Reza-E-Rabby, T. Roosendaal, W. Daye, T. Pelletiers, S. Mathaudhu, N. Overman, High ductility aluminum alloy made from powder by friction extrusion, Materialia 6 (2019) 100260, https://doi.org/10.1016/j.mtla.2019.100260.

[3] Y.J. Li, W.Z. Tao, Y.S. Yang, Grain refinement of Al–Cu alloy in low voltage pulsed magnetic field, J. Mater. Process. Technol. 212 (2012) 903–909.

[4] I.Y. Timoshkin, K.V. Nikitin, V.I. Nikitin, V.B. Deev, Influence of treatment of melts by electromagnetic acoustic fields on the structure and properties of alloys of the Al–Si system, Russ. J. Non-Ferrous Metals 57 (2016) 419–423, https://doi.org/10.3103/S1067821216050163.

[5] W. Muhammad, J. Kang, A.P. Brahme, U. Ali, J. Hirsch, H. Brinkman, O. Engler, R.K. Mishra, K. Inal, Bendability enhancement of an age-hardenable aluminum alloy: Part I — relationship between microstructure, plastic deformation and

fracture, Mat. Sci. Eng. A-Struc. 753 (2019) 179–191, https://doi.org/10.1016/j.msea.2019.03.053.
[6] S. Beroual, Z. Boumerzoug, P. Paillard, Y. Borjon-Piron, Effects of heat treatment and addition of small amounts of Cu and Mg on the microstructure and mechanical properties of Al-Si-Cu and Al-Si-Mg cast alloys, J. Alloy. Comp. 784 (2019) 1026–1035, https://doi.org/10.1016/j.jallcom.2018.12.365.
[7] M.T. Di Giovanni, E.A. Mørtsell, T. Saito, S. Akhtar, M. Di Sabatino, Y. Li, E. Cerri, Influence of Cu addition on the heat treatment response of A356 foundry alloy, Mater. Today. Com. 19 (2019) 342–348, https://doi.org/10.1016/j.mtcomm.2019.02.013.
[8] Q. Wang, X. Rui, Q. Wang, Y. Bai, Z. Du, W. Niu, W. Wang, K. Wang, Y. Gao, Bonding and wear behaviors of supersonic plasma sprayed Fe-based coatings on Al-Si alloy substrate, Surf. Coat. Technol. 367 (2019) 288–301, https://doi.org/10.1016/j.surfcoat.2019.04.003.
[9] S.V. Panin, I.V. Vlasov, V.P. Sergeev, P.O. Maruschak, R. Sunder, B.B. Ovechkin, Fatigue life improvement of 12Cr1MoV steel by irradiation with Zr+ ion beam, Int. J. Fatigue 76 (2015) 3–10, https://doi.org/10.1016/j.ijfatigue.2014.10.011.
[10] N. Kang, M.E. Mansori, A new insight on induced-tribological behaviour of hypereutectic Al-Si alloys manufactured by selective laser melting, Tribol. Int. (2019), https://doi.org/10.1016/j.triboint.2019.04.035.
[11] S. Mahanty, Gouthama, Surface modification of Al–Si alloy by excimer laser pulse processing, Mater. Chem. Phys. 173 (2016) 192–199, https://doi.org/10.1016/j.matchemphys.2016.02.001.
[12] A. Viswanathan, D. Sastikumar, H. Kumar, A.K. Nath, Laser processed TiC–$Al_{13}Fe_4$ composite layer formation on Al–Si alloy, Opt. Lasers Eng. 50 (9) (2012) 1321–1329, https://doi.org/10.1016/j.optlaseng.2012.02.013.
[13] C. Zijin, L. Yong, W. Hong, Z. Weidong, G. Wei, T. Huiping, L. Nan, Microstructures and wear properties of surface treated Ti–36Nb–2Ta–3Zr–0.35O alloy by electron beam melting (EBM), Appl. Surf. Sci. (2015) 2347–2354, https://doi.org/10.1016/j.apsusc.2015.09.240.
[14] P. Yua, M. Yana, D. Tomus, C.A. Briced, C.J. Bettles, B. Muddle, M. Qiane, Microstructural development of electron beam processed Al-3Ti-1Sc alloy under different electron beam scanning speeds, Mater. Char. 143 (2018) 43–49, https://doi.org/10.1016/j.matchar.2017.09.005.
[15] F. Yang, Q. Qin, T. Shi, C. Chen, Z. Guo, Surface strengthening aluminum alloy by in-situ TiC-TiB_2 composite coating, Ceram. Int. 45 (4) (2019) 4243–4252, https://doi.org/10.1016/j.ceramint.2018.11.096.
[16] Y. Li, P. Zhang, P. Bai, L. Wu, B. Liu, Z. Zhao, Microstructure and properties of Ti/TiBCN coating on 7075 aluminum alloy by laser cladding, Surf. Coat. Technol. 334 (2018) 142–149, https://doi.org/10.1016/j.surfcoat.2017.11.034.
[17] S. Konovalov, I. Komissarova, Yu Ivanov, V. Gromov, D. Kosinov, Structural and phase changes under electropulse treatment of fatigue-loaded titanium alloy VT1-0, J. Mater. Sci. Technol. 8 (1) (2019) 1300–1307.
[18] YuF. Ivanov, V.E. Gromov, S.V. Konovalov, D.V. Zagulyaev, E.A. Petrikova, A.P. Semin, Modification of structure and surface properties of hypoeutectic silumin by intense pulse electron beams, Prog. Phys. Met. 19 (2018) 195–222, https://doi.org/10.15407/ufm.19.02.195.
[19] B.J. Inkson, Scanning electron microscopy (SEM) and transmission electron microscopy (TEM) for materials characterization, in: G. Hübschen, I. Altpeter, R. Tschuncky, H. Herrmann (Eds.), Materials Characterization Using Nondestructive Evaluation (NDE) Methods, Woodhead Publishing, 2016, pp. 17–43.
[20] R.F. Egerton, Physical Principles of Electron Microscopy. An Introduction to TEM, SEM, and AEM, Springer US, Berlin, 2005.
[21] Challa S.S.R. Kumar, Transmission Electron Microscopy Characterization of Nanomaterials, Springer-Verlag Berlin Heidelberg, 2014.
[22] C.B. Carter, D.B. Williams, Transmission Electron Microscopy; Diffraction, Imaging, and Spectrometry, Springer International Publishing, Switzerland, 2016.
[23] J. Kawalko, P. Bobrowski, P. Koprowski, A. Jarzebska, M. Bieda, M. Lagoda, K. Sztwiertnia, Microstructure evolution of CP titanium during deformation in KoBo process followed by cold rolling, J. Alloy. Comp. 707 (2016) 298–303, https://doi.org/10.1016/j.jallcom.2016.11.202.